

SAMPLE SCALE TESTING METHOD TO PREVENT COLLAPSE OF PLASTIC LINERS IN COMPOSITE PRESSURE VESSELS

P. Blanc-Vannet^{1*}, P. Papin¹, M. Weber¹, P. Renault¹, J. Pepin², E. Lainé², G. Tantchou^{1,2},
S. Castagnet², J.-C. Grandidier²

¹ Air Liquide Research and Development, 1 Chemin de la porte des loges, BP 126 - 78354 Jouy en Josas, France, pierre.blanc-vannet@airliquide.com

² Département Physique et Mécanique des Matériaux, Institut Pprime, UPR 3346 CNRS – ENSMA – Université de Poitiers, Téléport 2, BP40109, 86961 Futuroscope, France

ABSTRACT

Type IV pressure vessels are commonly used for hydrogen on-board, stationary or bulk storages. When pressurized, hydrogen permeates through the materials and solves into them. Emptying then leads to a difference of pressure at the interface between composite and liner, possibly leading to a permanent deformation of the plastic liner called “collapse” or “buckling”. This phenomenon has been studied through French funded project Colline, allowing to better understand its initiation and long-term effects. This paper presents the methodology followed, using permeation tests, hydrogen decompression tests on samples, and gas diffusion calculation in order to determine safe operating conditions, such as maximum flow rate or residual pressure level.

NOMENCLATURE

1.0 INTRODUCTION

Composite pressure vessels are nowadays a mature way of storing compressed hydrogen. The combination of low weight and high mechanical strength make them particularly suitable for applications requiring high quantities of gas in a reduced and transportable volume, such as automotive fuel tanks or gas transportation trailers [1]. When it comes to deep cycles at very high pressures – typically 70 MPa – the liner is often made of polymer, in order to avoid hydrogen embrittlement of metals. Most frequently used polymers are polyethylene and polyamides, depending on the specifications for the final vessel. The method for assembling the liner together with the metallic bosses and with the composite shell is for the manufacturer to choose. In particular, the liner can be glued to the composite shell or left free to move inside it.

The permeation of gases through polymers is a well known phenomenon [2]. Gas molecules penetrate into the polymer, increasing the space between the molecules and reducing the intermolecular bonding; which further increases the permeation rate until equilibrium is reached. In particular, this leads to the phenomenon known as “buckling collapse” of polymeric liners in the oil and gas pipeline industry: gas accumulates at the region between the liner and the tube wall, applying a pressure on the external surface of the liner which, when the tube is rapidly emptied (for example in case of maintenance), leads to large deformation of the liner [3]. It has been shown that, depending on the thickness-to-diameter and yield stress-to-stiffness ratios, the collapse can appear either before or after plastic deformation of the liner [4]. This has led to intensive efforts to improve the modelling of the temperature and time dependence of polymers behaviour [5, 6, 7, 8].

More recently, the same phenomenon has been evidenced by depressurisation tests on hydrogen composite cylinders. A research project funded by the French national research agency (ANR) was started, in order to investigate the operating conditions leading to liner collapse and to estimate its long-term effects on liners durability [9, 10]. Within this project, decompression tests were performed on small 70 MPa cylinders comprising a polymer liner glued to the composite shell. Permeation tests at 70 MPa were performed on liner samples, and the collapse phenomenon was reproduced on representative samples (liner layer bonded to a composite plate) in order to investigate influent parameters.

This paper presents the cylinder-scale experimental part of the project. The parameters allowing to calculate the gas diffusion through the liner were extracted from the permeation tests, in order to predict the maximal pressure at the interface between liner and composite. This interface pressure is then compared to the decompression tests results and to the apparition or not of collapse.

2.0 EXPERIMENTAL SETUPS

2.1 Permeation tests

Permeation tests were carried out on samples from the different materials involved, in order to predict the hydrogen solubility and diffusion through the vessel's wall. A dedicated test bench able to carry out permeation tests a 70 MPa of hydrogen was used (Fig. 1). Samples are disks of diameter 40 mm, and of three possible thicknesses: 2.1 mm or 3.1 mm or 3.6 mm. They were machined from plates made of the same materials as the pressure vessel. Though the plates were rectangular, the composite layer was filament-wound in order to be as close as possible to the real vessel.

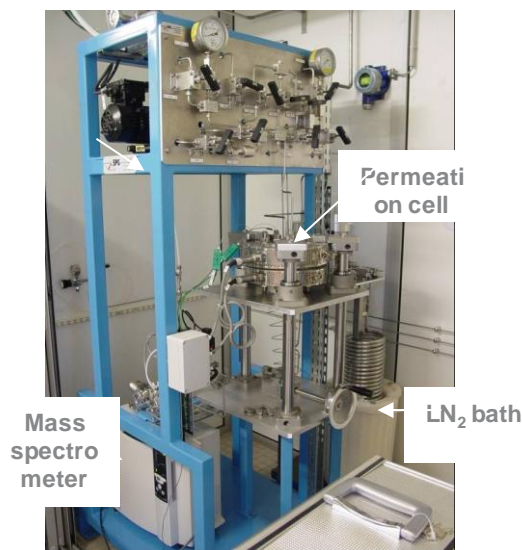


Figure 1 70 MPa hydrogen permeation test bench

Samples of all involved materials were tested: liner, epoxy resin alone, carbon fibre / epoxy composite. Tests were carried out at different pressures: 5 MPa, 8 MPa, 18 MPa, 35 MPa, 45 MPa, 70 MPa; and different temperatures: 27 °C and 55 °C. The samples are exposed to hydrogen pressure on one side. A liquid nitrogen based heat exchanger is used to regulate the temperature during hydrogen pressure increase. The gas which permeates to the other side is extracted and analysed using mass spectrometry. The flow of hydrogen through the sample is recorded as a function of time.

From the evolution of the hydrogen flow, the values of permeability, diffusion and solubility parameters are extracted as described in [11]. For confidentiality reasons, their values are not displayed in this paper. They are used to estimate the hydrogen flow through the actual pressure vessels and calculate the pressure at the liner-composite interface during emptying tests, as will be presented in section 3.0.

2.2 Rapid decompression tests

The pressure vessels used for this work were manufactured especially for R&D purposes, and are not a commercially available object. They were designed according to standards for transportable cylinders [12], i.e. targeting a burst pressure of 3 times the service pressure of 70 MPa. The first design led to an actual burst pressure of 196.3 (+/-3) MPa; which was found acceptable for the research purpose even

though it does not comply with the standard – a second design iteration was not performed in order to save time and costs. The liner has a thickness-over-external diameter ratio (t/D) of 0.019.

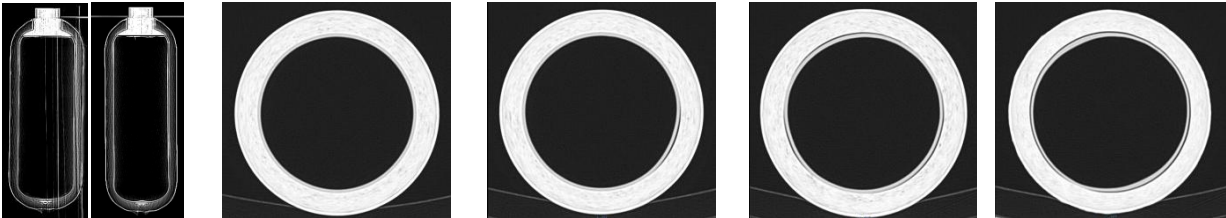
Twelve cylinders were submitted to rapid hydrogen decomposition tests. They were pressurized to either 50% of 100% state-of-charge, corresponding to 35 MPa or 70 MPa at 15 °C. The permeation rate through the vessels could not be measured; it was numerically estimated to 48 h, so a minimal dwelling time of one week was observed after pressurisation. During this dwelling time the temperature was set to 40 °C in order to even more accelerate the reaching of the steady state. The temperature was then decreased to 25 °C and, after enough time to ensure a uniform temperature, the vessels were emptied. Due to the size of the climatic chamber, a maximum of four vessels were tested at the same time.

In order to avoid damaging the liners, the gas temperature must be kept above -40 °C at all times. The corresponding maximal flow rate was numerically estimated to be around 7 bar/min using a simplified OD model [13], and temperature sensors were placed on the vessels to monitor the temperature decrease of the external wall. The experimental setup can be observed in Fig 2.



Figure 2 Picture of the experimental setup with four vessels inside the climatic chamber. A microphone and a thermocouple are placed on the external surface of each vessel.

CT scan examination of the cylinders was performed after a minimum waiting time of one week after the end of emptying. This time is expected to be sufficient for all mechanical stresses to be relieved. As the CT scan device is located in another area, it was not possible to precisely master the time between the end of emptying and the examination, so it was decided that all observations should be made at an “infinite” time compared to the liner’s response to ensure their consistency. Three of the twelve cylinders used were also CT scanned before testing to provide the initial state. The resulting “initial state” CT scans are displayed on Fig 3. Each line represents a single pressure vessel, and for each one the different cross-sectional views are taken at different heights.



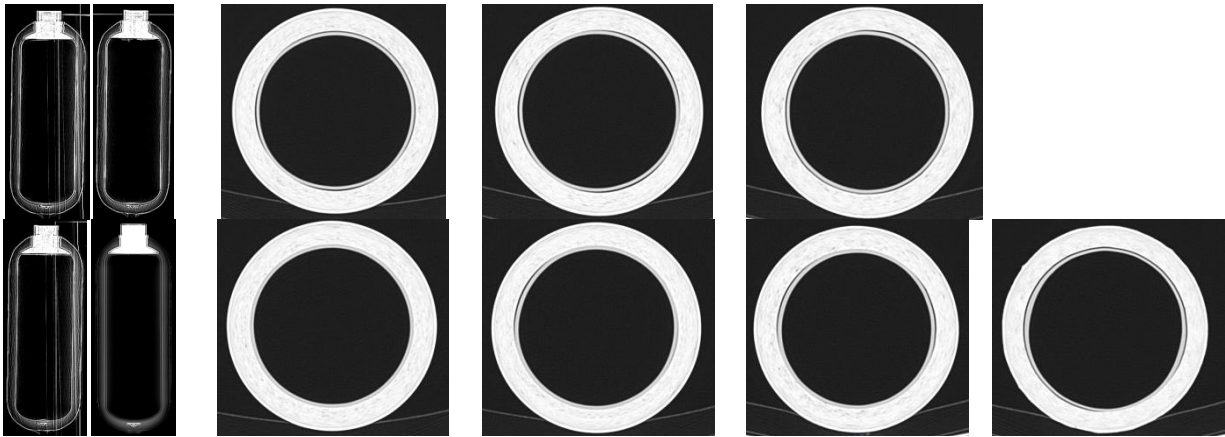


Figure 3 CT scans of three pressure vessels (one per line) before being submitted to decompression tests. From top to bottom, vessels numbers are 10, 11, 12

At this point it is interesting, even though the pressure vessels have been submitted to nothing else than hydraulic proof test just after manufacturing (ca. 30 s hold at 105 MPa hydraulic pressure – a mandatory step to ensure safety), to observe that on all three of them there are some areas with a small gap between liner and composite. This is surprising, as glue is applied on the liner to ensure a good bonding with the first composite layer, and does not seem to be due to the CT scan resolution as it is observed only locally. Whether it is due to manufacturing, with a winding made before the polymer has finished shrinking, or due to hydraulic proof test, is unclear at this point. Anyway, this initial state should be kept in mind when analysing the post-decompression state.

3.0 RESULTS AND DISCUSSION

3.1 Prediction of the maximal external pressure applied on the liner

Using Henry's law and the solubility parameter determined during permeation tests, the quantity of hydrogen solved in the materials can be calculated for a given level of internal pressure. The dwelling at high pressure is sufficient to reach the steady state. The mesh used for the calculation of the pressure gradient through the wall is displayed on Fig 4, for an internal pressure of 87.5 MPa. Such pressure corresponds to the maximal accepted inside the vessel at the end of filling. It can be observed that, due to the difference of solubility between liner and composite materials, there is almost no pressure gradient through the liner depth.

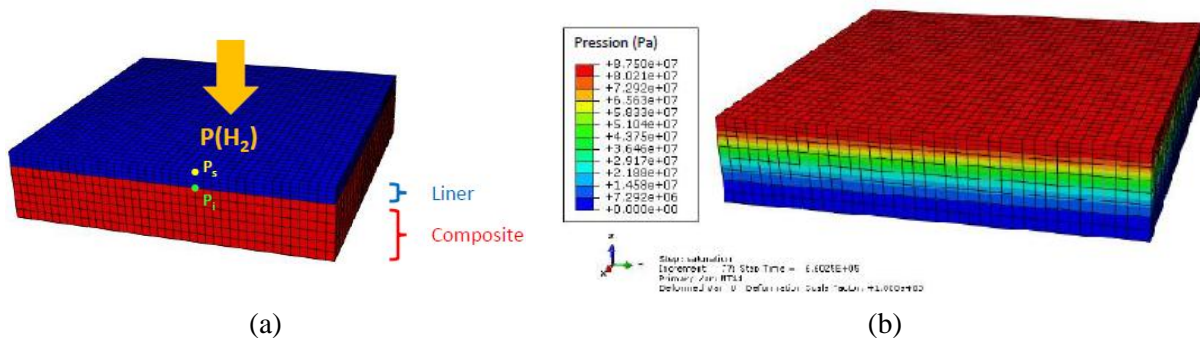


Figure 4 (a) Mesh used for the diffusion calculation, (b) Pressure gradient through the liner and composite for an internal pressure of 87.5 MPa

From this steady state, a gas diffusion calculation is performed in order to calculate the evolution of the pressure at liner-composite interface (P_i , green point on Fig 4(a)) during the decompression step. The pressure applied on the internal liner surface (P_s , yellow point on Fig 4(a)) is decreased at a constant rate. Calculations were made with decompression rate from 0.007 MPa/min to 0.7 MPa/min. For each case, the pressure applied on the liner from the outside ($\Delta P_{H2} = P_i - P_s$) is plotted as a function of the internal pressure P_i on Fig 5. On Fig 5(a) the initial internal pressure is 35 MPa, while on Fig 5(b) the initial internal pressure is 87.5 MPa.

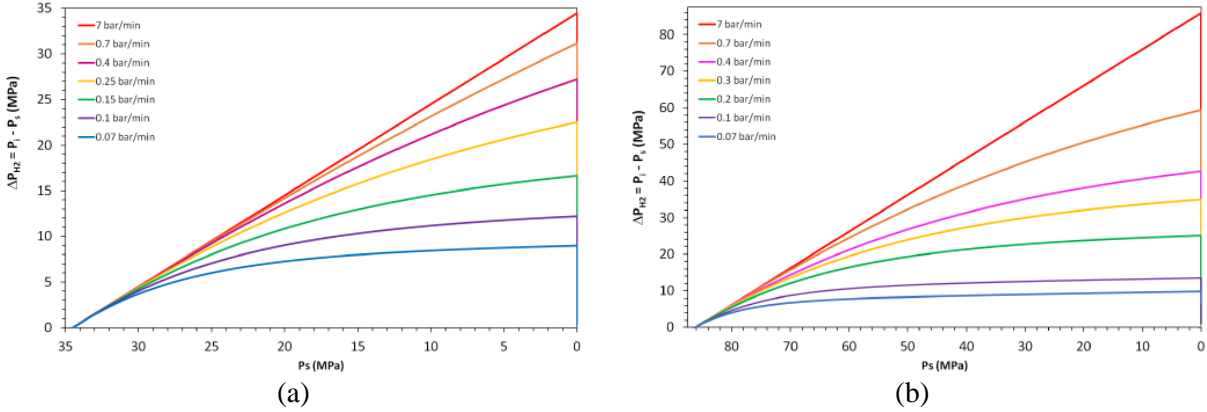


Figure 5 Evolution of the pressure applied from the outside of the liner (liner-composite interface pressure minus pressure inside the vessel, $P_i - P_s$) vs. internal pressure; during decompressions at 0.007 to 0.7 MPa/min; for initial internal pressures of (a) 35 MPa and (b) 87.5 MPa

It can be seen on Fig 5 that, when the emptying rate is high, the curves are almost linear. This means that the emptying of the vessel is very fast compared to the gas desorption from the materials: in this case, the pressure at liner-composite interface remains almost constant while the internal pressure is removed, and the maximal pressure applied from outside the liner is almost equal, at the end of emptying, to the initial pressure. On the other hand, when the emptying is slower, some gas has enough time to get out of the composite from the external open surface, which leads to a decrease of the liner-composite interface pressure. In this case, the curves are “bending” towards a lower maximal pressure.

At the end of emptying, the pressure applied on the liner from the liner-composite interface is ΔP_{max} , which variation with emptying flow rate are displayed on Fig 6 (for an initial pressure of 87.5 MPa and emptying rates of 0.7 MPa/min and 0.07 MPa/min) and in Table 1 for all calculation conditions.

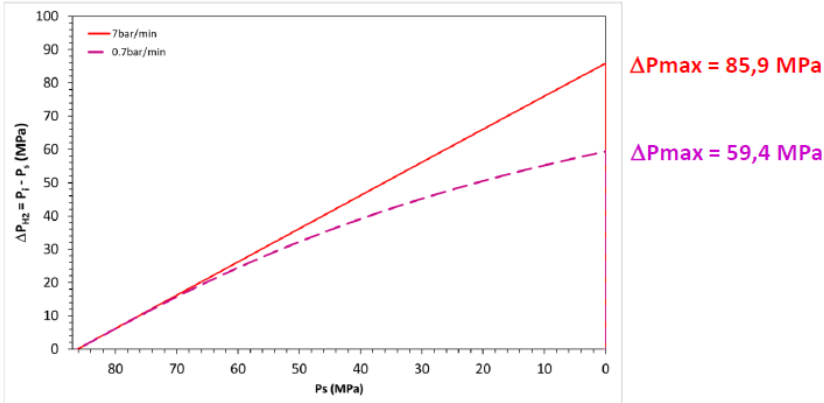


Figure 6 Maximal pressures applied from outside the liner, for initial pressure of 87.5 MPa and emptying rates of 0.7 and 0.07 MPa/min

Table 1 Maximal pressure applied from outside the liner in all calculation conditions

Initial pressure 35 MPa		Initial pressure 87.5 MPa	
Emptying rate	ΔP_{max}	Emptying rate	ΔP_{max}
0.007 MPa/min	9.0 MPa	0.007 MPa/min	10.0 MPa
0.01 MPa/min	12.4 MPa	0.01 MPa/min	12.7 MPa
0.015 MPa/min	16.5 MPa	0.02 MPa/min	24.8 MPa
0.025 MPa/min	22.5 MPa	0.03 MPa/min	34.6 MPa
0.04 MPa/min	27.1 MPa	0.04 MPa/min	42.4 MPa
0.07 MPa/min	31.1 MPa	0.07 MPa/min	59.4 MPa
0.7 MPa/min	34.2 MPa	0.7 MPa/min	85.9 MPa

The results gathered in Table 1 are also plotted on Fig 7, which displays ΔP_{max} as a function of emptying rate. It can be observed that when the emptying is faster than 0.1 MPa/min for an initial pressure of 35 MPa or faster than 0.25 MPa/min for an initial pressure of 87.5 MPa, the gas diffusion can be neglected. In this case, it can simply be assumed that ΔP_{max} is equal to the initial internal pressure.

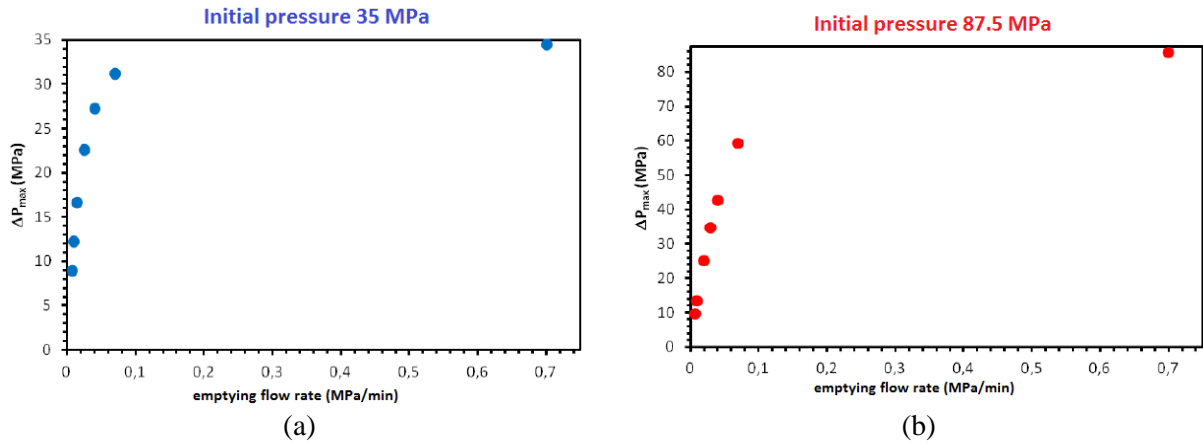


Figure 7 Maximal pressure applied from outside the liner as a function of emptying flow rate, for initial pressures of (a) 35 MPa and (b) 87.5 MPa

3.2 Results of the decompression tests

This section presents the results obtained after fast decompression tests on a total of eight different pressure vessels. For each vessel, the first picture is a vertical view and the following ones are cross-sectional views taken at the most significant places (from bottom to top). The cylinders were CT scanned by batches of 2 to 4, and scans made on different days exhibit small variations in terms of contrast.

The first four vessels were initially pressurised at 35 MPa and emptied at respectively 0.015, 0.03, 0.07 and 0.7 MPa/min until reaching atmospheric pressure, and all the corresponding CT scan pictures are gathered in Table 2. Then, the results for an initial pressure of 70 MPa are gathered in Table 3. Three vessels were pressurised at 70 MPa and emptied at respectively 0.01, 0.07 and 0.7 MPa/min down to atmospheric pressure. In order to mimic real operating life of such vessels, another one was emptied at 0.7 MPa/min (approximately maximal allowable flow rate) from 70 MPa (service pressure) to 2 MPa (residual pressure level kept in vessels). It was left at 2 MPa for 72h before being emptied down to atmospheric pressure at 0.7 MPa/min, which typically could happen in case of maintenance of

vessel or valves. In this latter case, the maximal pressure applied from outside the liner can be estimated to be around 65 MPa at the end of the first defueling step.

From all the results, it can be observed that there is a strong relationship between the maximal pressure applied on the external surface of the liner and the severity of the collapse created. For both initial pressures, the lower flow rates, which lead to lower ΔP_{max} , do not create significant liner collapse ($\Delta P_{max} \leq 25$ MPa). For intermediate levels ($30 \text{ MPa} \leq \Delta P_{max} \leq 60$ MPa), significant evidence of liner collapse are visible on the CT scans, with increased gaps between liner and composite. In one of the cases (35 MPa, 0.7 MPa/min i.e. $\Delta P_{max} = 34$ MPa) there is also a residual buckling near the closed dome. Highest levels of ΔP_{max} , achieved only when starting from 70 MPa and with quickest emptying, lead to extreme collapse modes: the liner remain permanently deformed from one dome to the other, and in one case exhibits very irregular shape.

It should also be noted that with standard values for the material used (taken from Idemat 2003 database), the yield-to-stiffness ratio $\sigma_y/E' = (1 - \nu^2) \cdot \sigma_y/E$ (where σ_y is the yield stress, E the elastic modulus and ν the Poisson's ratio) of the liner is between 0.0187 and 0.0147. According to [4], such liner design with $t/D = 0.019$ is in the "inelastic collapse" area, meaning that the collapse is expected to occur after the onset of plastic deformation.

In the most severe cases such as the one reproduced in Fig 8, an effect seems to be visible also in the composite layer. Multiple black spots can be seen, and they could result from initial porosities which got worsened by the hydrogen desorption. Still, this cannot be completely assured, as the variation in contrast from one CT scan to another are disturbing the observations. Some quite long cracks can also be observed on Fig 8 which could be explained the same way. Finally, there is also a gap between the carbon fibre layer and the external glass fibre layer – whether this is also an effect of decompression or an artifact of CT scan is unclear. The evolution of defects in the composite shell and the liner of a pressure vessel submitted to successive rapid decompression should be studied further.

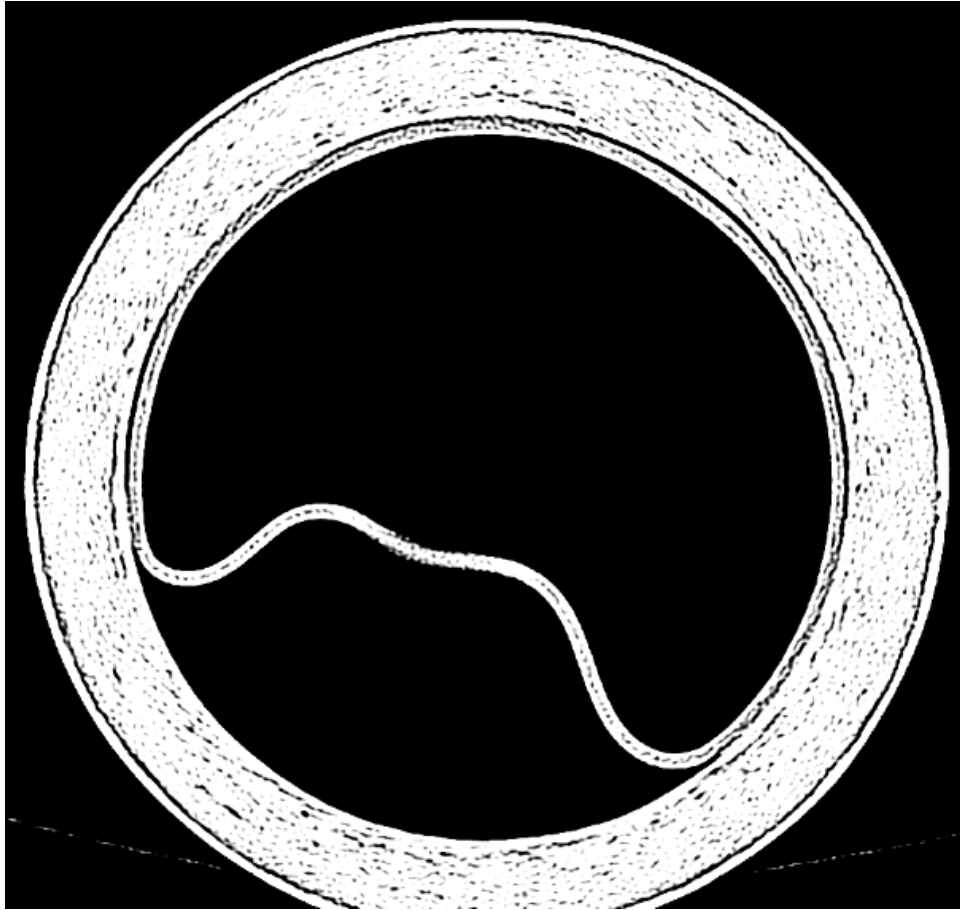


Figure 8 CT scan picture of the vessel #02 - emptied at 0.7 MPa/min from 70 MPa to 2 MPa, then from 2 MPa to atmospheric pressure after 72h. A very important collapse is present from one dome to the other, with irregular shape. Multiple cracks can be observed in the composite layer.

In Table 4, two vessels which exhibited no collapse in the previous phase were then used a second time in conditions (35 MPa – 0.7 MPa/min) in order to assess the reproducibility of the collapse in this specific case. The first vessel tested (#07) exhibits important signs of liner collapse: the gaps between liner and composite are wider than in the initial state, and an area at the bottom of the cylindrical part remains permanently buckled. On the other hand, the two other vessels (#10 and #11) do not present important signs of collapse. The gaps are slightly wider than they were initially (Fig 3) and after the first slower emptying (Table 2), but not as wide as they are in vessel #07. There is no specific area with large permanent liner deformation. There are two potential explanations for such difference between the vessels: (i) considering the initial state, it can be assumed that there is variability in the quality of the liner-composite bonding, vessel #07 having a weaker interface in some spots, hence the widely deformed area; and/or (ii) the first emptying of vessels #10 and #11, respectively at 0.015 and 0.030 MPa/min, has an influence on the liner behaviour during the second emptying at 0.7 MPa/min. Unfortunately the number of cylinders available for testing did not permit to explore this any further.

Table 2 Results of the decompression tests with initial pressure 35 MPa



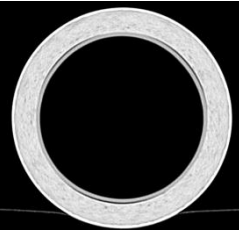
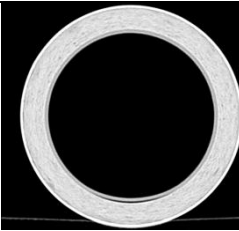
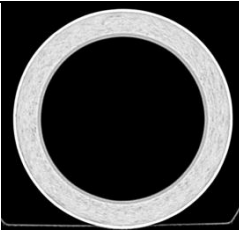


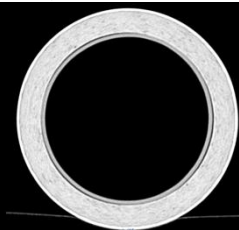
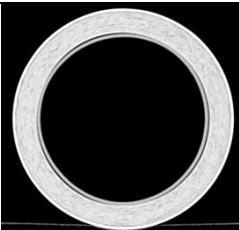
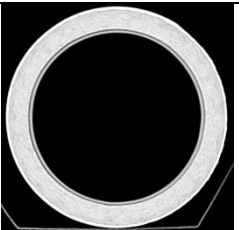

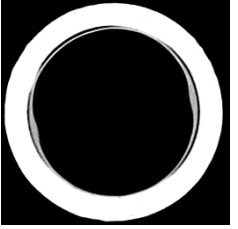
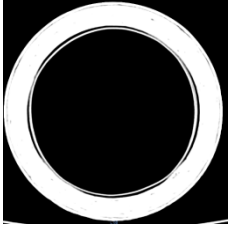
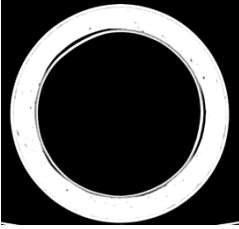
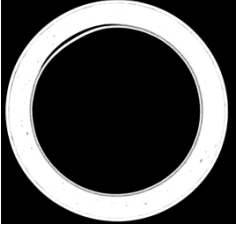

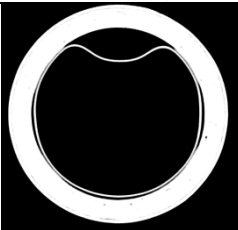
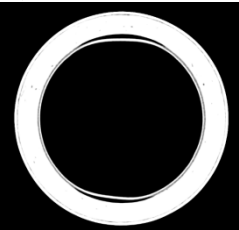
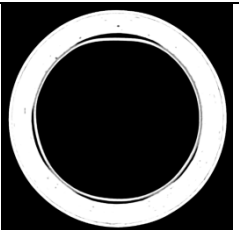
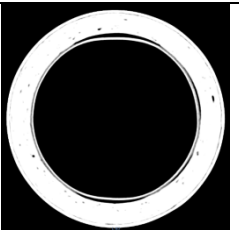
35 MPa – 0.015 MPa/min (Vessel #10)				
				
<p>No liner collapse is observed on this vessel. Small gaps are sometimes visible between liner and composite, but there does not seem to be any difference with the initial state displayed on Fig 3.</p> <p>The maximal pressure applied from outside the liner is estimated at $\Delta P_{max} = 16.5$ MPa according to Table 1.</p>				
35 MPa – 0.030 MPa/min (Vessel #11)				
				
<p>No liner collapse is observed on this vessel. Small gaps are sometimes visible between liner and composite, but there does not seem to be any difference with the initial state.</p> <p>ΔP_{max} is estimated to 25 MPa</p>				
35 MPa – 0.07 MPa/min (Vessel #08)				
				
<p>This vessel exhibits signs of liner collapse. The gaps between liner and composite seem to be a bit more marked than in the initial state (though there was no initial CT scan on this specific cylinder). As the CT scan is performed after one week, it can be expected that larger liner deformation were present shorter after the end of emptying.</p> <p>The increased liner thickness in the first picture is not due to collapse but to liner manufacturing process.</p> <p>ΔP_{max} is estimated to 31 MPa</p>				
35 MPa – 0.7 MPa/min (Vessel #07)				
				
<p>Important liner collapse is visible on this vessel, even a long time after the end of emptying. Gaps between liner and composite are wider, and an area at the bottom of the cylinder remains permanently deformed. Some black spots appear in the composite layer.</p> <p>ΔP_{max} is estimated to 34 MPa</p>				

Table 3 Results of the decompression tests with initial pressure 70 MPa



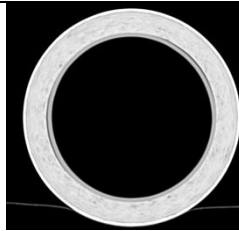
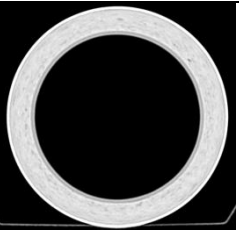
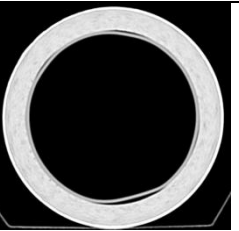

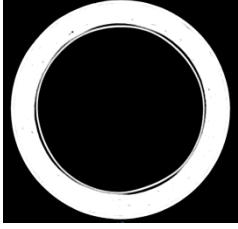
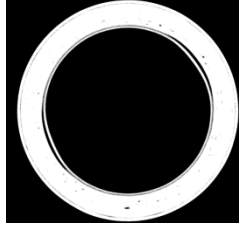
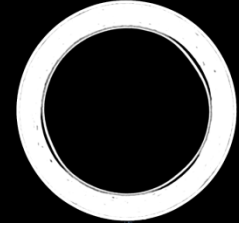
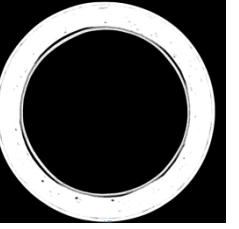






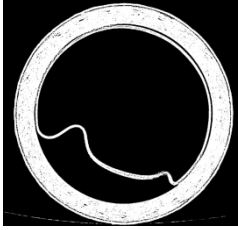
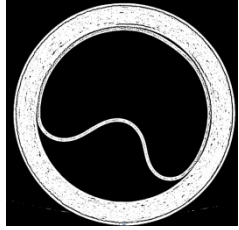
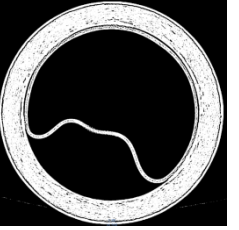
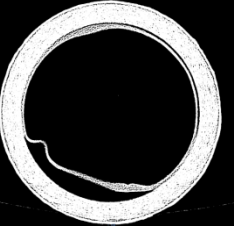

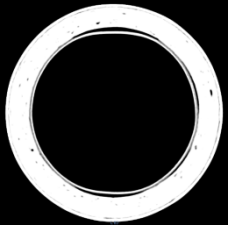
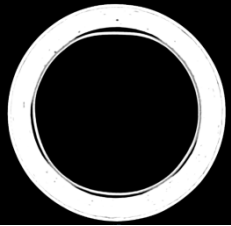
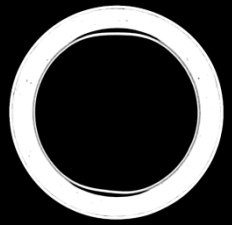
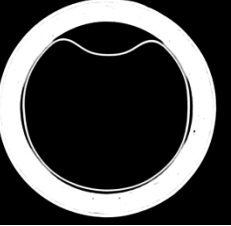

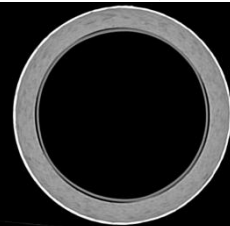
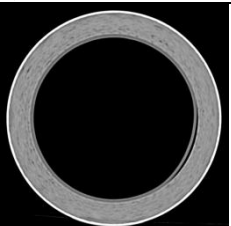
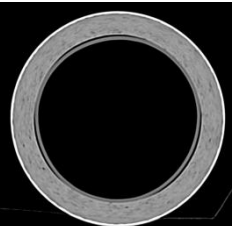
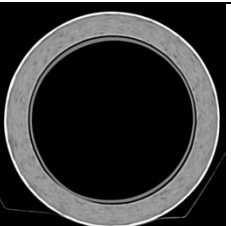

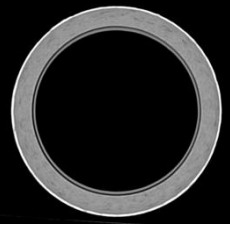
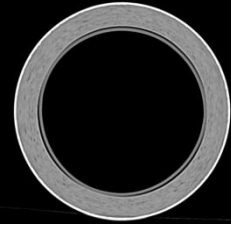
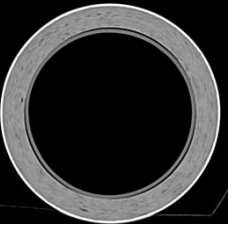
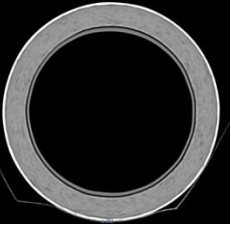
70 MPa – 0.01 MPa/min (Vessel #12)				
				
<p>Most of this vessel does not exhibit important signs of liner collapse. In the bottom of the cylindrical part (last picture), a wider gap is visible, which probably corresponds to a spot with initially weaker bonding. The initial width of the gap is unknown but it has likely been worsened by emptying.</p> <p>Calculations of ΔP_{max} have not been carried out for this case, but according to the other results it can be estimated around 20 MPa.</p>				
70 MPa – 0.07 MPa/min (Vessel #05)				
				
<p>This vessel is very similar to #08. Gaps between liner and composite are slightly wider than in initial state. Some black spots are visible in the composite layer.</p> <p>Calculations of ΔP_{max} have not been carried out for this case, but according to the other results it can be estimated around 50 MPa.</p>				
70 MPa – 0.70 MPa/min (Vessel #04)				
				
<p>This vessel exhibits extreme liner collapse with very important permanent deformation. It can be seen on the vertical picture that on one side the buckled shape goes from one dome to the other, whereas on the other side a second collapse stretches along the lower half.</p> <p>ΔP_{max} has not been calculated but is estimated around 68 MPa.</p>				
70 MPa – 0.70 MPa/min (Vessel #02) - Defueling paused at 2 MPa for 72 hours				
				
<p>This vessel exhibits extreme liner collapse. Unlike the previous one, the collapse is only on one side and its shape is very irregular from one dome to the other. Multiple black spots and even long cracks can be seen in the composite.</p> <p>ΔP_{max} has not been calculated but is estimated around 65 MPa.</p>				

Table 4 Reproducibility tests for initial pressure 35 MPa, emptying rate 0.7 MPa/min

35 MPa – 0.7 MPa/min (Vessel #07)				
				
<p>Important liner collapse is visible on this vessel, even a long time after the end of emptying. Gaps between liner and composite are wider, and a buckled area at the bottom of the cylinder remains permanently deformed.</p> <p>ΔP_{max} is estimated to 34 MPa</p>				
35 MPa – 0.7 MPa/min (Vessel #10)				
				
35 MPa – 0.7 MPa/min (Vessel #11)				
				
<p>These two vessels do not show very important signs of collapse. Compared to their initial state – Fig 3 – and their state after slower emptying – Table 2 – the gaps appear a bit wider, but not in the same extent as they are for vessel #07. Moreover, there is no specific buckled area.</p>				

4.0 CONCLUSIONS

A series of pressure vessels prototypes, manufactured according to transportable gas cylinders standards for a service pressure of 70 MPa, was submitted to hydrogen emptying tests representative of service conditions. They were filled up to 50% or 100% state of charge, left full for a week, then emptied with flow rates up to 0.7 MPa/min. For the highest initial pressures and flow rates, extreme collapse with liner deformed from one dome to the other was observed by CT scan at least one week after the end of defueling.

Permeation tests were made on samples of the different materials of the vessel, and the parameters required to perform gas diffusion calculations were extracted. This allowed calculating the pressure at the liner-composite interface during the defueling, and the maximal pressure applied on the liner from its external surface. It was evidenced that this maximal pressure, which depends on initial and final pressures and on emptying flow rate, correlates to the severity of the collapse observed. Numerical simulations can then be a way to investigate liner materials and designs limiting the appearance of liner collapse in regular operating conditions.

In the most severe cases, it has also been observed that the hydrogen decompression seems to affect the composite shell. It is possible that if porosities or cracks are present in the composite due to manufacturing, their sizes can be increased by hydrogen desorption. The long-term effects of repeated hydrogen cycles, each one with a long dwelling at high pressure, on the burst pressure or cycling performance of composite pressure vessels should be studied further; especially when the composite layer has an important void content.

5.0 ACKNOWLEDGMENTS

This work was performed thanks to the funding of the Agence Nationale de la Recherche (ANR) in the project Colline - <http://www.agence-nationale-recherche.fr/?Project=ANR-13-RMNP-0007>

6.0 REFERENCES

- [1] H. Barthélémy, M. Weber and F. Barbier, "Hydrogen storage: Recent improvements and industrial perspectives," *International Journal of Hydrogen Energy*, 2016.
- [2] S. A. Stern and J. R. Fried, "Permeability of polymers to gases and vapors," in *Physical Properties of Polymers Handbook*, Springer, 2007, pp. 1033-1047.
- [3] D. Glock, "Behavior of liners for rigid pipeline under external water pressure and thermal expansion," *Der Stahlbau*, vol. 46, no. 7, pp. 212-217, 1977.
- [4] K. M. El-Sawy, "Inelastic stability of tightly fitted cylindrical liners subjected to external uniform pressure," *Thin-Walled Structures*, 2001.
- [5] E. M. Arruda, M. C. Boyce and R. Jayachandran, "Effects of strain rate, temperature and thermo-mechanical coupling on the finite strain deformation of glassy polymers," *Mechanics of Materials*, vol. 19, no. 2-3, pp. 193-212, 1995.
- [6] J. S. Bergström and M. C. Boyce, "Constitutive modeling of the large strain time-dependent behavior of elastomers," *Journal of the Mechanics and Physics of Solids*, vol. 46, no. 5, pp. 931-954, 1998.
- [7] J. S. Bergström, C. M. Rimnac and S. M. Kurtz, "An augmented hybrid constitutive model for simulation of unloading and cyclic loading behavior of conventional and highly crosslinked UHMWPE," *Biomaterials*, 2004.
- [8] J. S. Bergström and J. E. Bischoff, "An Advanced Thermomechanical Constitutive Model for UHMWPE," *International journal of structural changes in solids*, vol. 2, no. 1, pp. 31-39, 2010.
- [9] P. Blanc-Vannet, P. Papin, M. Weber, G. Tantchou, J. Pepin, E. Lainé, J.-C. Grandidier, S. Castagnet and C. Langlois, "Definition of representative samples to study hydrogen type IV pressure vessels liner collapse phenomenon," in *21st World Hydrogen Energy Conference*, Zaragoza, Spain, 2016.
- [10] G. Tantchou, S. Castagnet, M. Weber, P. Blanc-Vannet and P. Papin, "Experimental and numerical study of the durability of polymer liners for hyperbaric H₂-composite vessels," in *10th International Conference on the Mechanics of Time Dependent Materials*, Paris, France, 2016.
- [11] B. R. Murray, S. B. Leen, C. Semprinoschnig and C. M. O Bradaigh, "Helium permeability of polymer materials as liners for composite overwrapped pressure vessels," *Journal of Applied Polymer Science*, 2016.
- [12] EN 12245, *Transportable gas cylinders - Fully wrapped composite cylinders*, 2009.
- [13] T. Bourgeois, F. Ammouri, M. Weber and C. Knapik, "Evaluating the temperature inside a tank during a filling with highly-pressurized gas," *International Journal of Hydrogen Energy*, vol. 40, no. 35, p. 11748–11755, 2015.